

## Long-term correlations in stochastic systems with extended time-delayed feedback

J. Pomplun,<sup>1</sup> A. G. Balanov,<sup>2</sup> and E. Schöll<sup>1</sup>

<sup>1</sup>*Institut für Theoretische Physik, Technische Universität Berlin, Hardenbergstrasse 36, D-10623 Berlin, Germany*

<sup>2</sup>*School of Physics and Astronomy, University of Nottingham, University Park, Nottingham NG7 2RD, United Kingdom*

(Received 20 November 2006; published 2 April 2007)

The effects of a feedback with multiple time delays on noise-induced dynamics are studied in a nonlinear system close to the Hopf instability. We show analytically and numerically that such a feedback creates two distinct time scales, which can be tuned independently by the feedback parameters. In this way, the coherence of noise-induced oscillations can be drastically improved, and an arbitrarily large correlation of oscillations can be achieved without inducing a bifurcation. This opens up new perspectives for control of stochastic dynamical systems.

DOI: [10.1103/PhysRevE.75.040101](https://doi.org/10.1103/PhysRevE.75.040101)

PACS number(s): 05.40.Ca, 05.45.Gg

With the discovery of stochastic [1] and coherence resonance phenomena [2,3] the role of random fluctuations in nature had to be seriously reassessed. It was found that in nonlinear systems the energy of noise can be counterintuitively utilized for enhancement or even generation of ordered motion. Such a constructive influence of noise appears to be important in many areas of science, see [4,5] for recent reviews. Once the prominent role of noise-induced effects is understood, it appears very attractive to control those, i.e., deliberately change their features. However, although the principles for controlling deterministic motion are quite well developed, the control of dynamics, which is strongly influenced by noise is still an open problem. One of the prospective ways of solving this problem seems to be the adaptation of methods for chaos control [6–8].

The effect of fluctuations is most conspicuous if the system is close to an instability. In this case, noise can drastically change the dynamics of the system, e.g., by creating new ordered dynamical patterns [5]. In this Rapid Communication we consider a nonlinear oscillator below a Hopf bifurcation, where an addition of noise leads to the appearance of quite regular oscillations, whose coherence depends upon the noise intensity. We analytically describe the effects of extended time-delayed feedback, which includes multiple delays, on noise-induced dynamics in the system. In particular, we demonstrate that such feedback can drastically improve long-term correlation of stochastic oscillations.

As a paradigmatic model we use the Van der Pol system with an extended time-delayed feedback loop  $F(t)$  in a form, which was earlier proposed for the control of deterministic chaos [9],

$$\begin{aligned} \dot{x} &= y, \\ \dot{y} &= (\varepsilon - x^2)y - \omega_0^2 x + D\xi(t) + F(t). \end{aligned} \quad (1)$$

Here  $F(t) \equiv K \sum_{\nu=0}^{\infty} R^{\nu} \{y[t - (\nu+1)\tau] - y(t - \nu\tau)\}$ ,  $\omega_0$  is the natural oscillation frequency,  $\varepsilon$  is the bifurcation parameter, which vanishes at the (supercritical) Hopf bifurcation, and  $x$  and  $y$  define a state of the system. The term  $D\xi(t)$  represents Gaussian white noise with zero mean and intensity defined by the parameter  $D$ :  $\langle \xi(t) \rangle = 0$ ,  $\langle \xi(t)\xi(t') \rangle = \delta(t-t')$ . The control force  $F(t)$  is an infinite sum of differences of the variable

$y$  at time  $t - (\nu+1)\tau$  and  $t - \nu\tau$  ( $\nu \in \mathbb{N}$ ) weighted with  $R^{\nu}$ . To assure that the sum converges, we restrict the memory parameter  $R$  to  $0 \leq R < 1$ . Experimentally, such a control scheme can be easily realized, e.g., with lasers coupled to an external Fabry-Pérot resonator [10]. For  $R=0$  we obtain the single-time delayed feedback scheme introduced by Pyragas [11]. With increasing  $R$  states of the system further in the past at times  $(t - \nu\tau)$  become more important. The parameter  $K$  represents the strength of extended delayed feedback. Note that the control force  $F$  can be written as the recursion  $F(t) = K[y(t - \tau) - y(t)] + RF(t - \tau)$ , which indicates a simple implementation of this feedback. In the following we fix the parameters  $\varepsilon = -0.01$  and  $\omega_0 = 1$ , where a stable focus at the origin  $(x, y) = (0, 0)$  is the only attractor in the deterministic system ( $D=0$ ). For  $D \neq 0$  the system exhibits noise-induced oscillations.

In order to quantify the coherence and time scales of those noisy oscillations, we introduce the normalized autocorrelation function (ACF) of  $y$ ,

$$\Psi_{yy}(s) = \sigma_{yy}^{-2} \langle (y(t-s) - \langle y \rangle)(y(t) - \langle y \rangle) \rangle, \quad (2)$$

with  $\sigma_{yy}^2 = \langle (y(t) - \langle y \rangle)^2 \rangle$  and the power spectral density

$$S_{yy}(\omega) = \lim_{T \rightarrow \infty} \frac{1}{2\pi T} \left| \int_0^T y(t) e^{-i\omega t} dt \right|^2. \quad (3)$$

The ACF of noise-induced oscillations in the Van der Pol system is a fast oscillating function with an exponentially decaying envelope [12,13]. We define the exponential correlation time  $t_e$  as the decay constant of this envelope. Thus, the larger  $t_e$ , the more regular is the dynamics. For  $R=0$  the ACF can be approximated by  $\Psi_{yy}(s) = \cos(\omega_0 s) \exp(-s/t_e)$ , and  $t_e \approx \frac{\pi}{2} t_{cor}$  holds with  $t_{cor} = \int_0^{\infty} |\Psi_{yy}(s)| ds$  [12,14].

However,  $R \neq 0$  leads to a qualitative change of the character of the ACF. Figure 1 shows that there are two time scales in the ACF: a slow exponential decay, which is already present in the case  $R=0$ , and a new fast time scale of correlation, which manifests itself in a sudden drop of the ACF within a very short time interval  $\Delta s$  comparable to the basic period of oscillation  $T_0 = 2\pi/\omega_0$ . To explain two characteristic time scales of the ACF we calculate the power spectral density  $S_{yy}(\omega)$ . Using the self-consistent mean-field

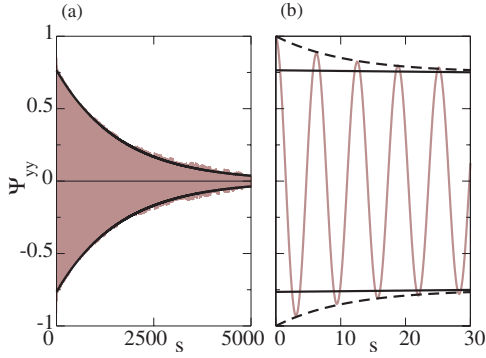


FIG. 1. (Color online) (a) Autocorrelation function  $\Psi_{yy}$  of the controlled Van der Pol system for  $R=0.9$ ,  $\tau=6.3$ ,  $K=0.2$ ,  $D=0.003$ . The fast oscillations (shading) are not resolved. (b) Blowup of the first 30 time units. Dashed line: short-time exponential decay. Solid line: long-time exponential envelope.

method of [13], it is possible to show that close to the Hopf bifurcation ( $|\varepsilon| \ll 1$ ) the dynamics of Eq. (1) can be approximately described by the linear equation

$$\dot{x} = y, \quad \dot{y} = \tilde{\varepsilon}y - \omega_0^2 x + D\xi(t) + F(t), \quad (4)$$

with the rescaled bifurcation parameter

$$\tilde{\varepsilon} = \varepsilon - \langle x^2 \rangle = \frac{\varepsilon}{2} \left( 1 + \sqrt{1 + \frac{2D^2}{\varepsilon^2 \omega_0^2}} \right). \quad (5)$$

In Fourier space the dynamic equations read  $-i\omega \hat{x} = \hat{y}$ ,  $-i\omega \hat{y} = \tilde{\varepsilon} \hat{y} - \omega_0^2 \hat{x} + D \hat{\xi} - K \hat{y}(1 - e^{i\omega\tau}) / (1 - R e^{i\omega\tau})$ , where  $\hat{x}(\omega)$ ,  $\hat{y}(\omega)$  are the Fourier transforms of  $x(t)$ ,  $y(t)$ . Note that for small noise intensity  $D \ll \omega_0 |\varepsilon|$ , we can set  $\tilde{\varepsilon} \approx \varepsilon$ . Taking into account that  $\langle \hat{y}^*(\omega) \hat{y}(\omega') \rangle = \delta(\omega - \omega') S_{yy}(\omega)$ , and  $\langle \hat{\xi}^*(\omega) \hat{\xi}(\omega') \rangle = \frac{1}{2\pi} \delta(\omega - \omega')$ , we obtain the spectrum

$$S_{yy}(\omega) = \frac{D^2}{2\pi [\omega^2 - \omega_0^2 + \alpha(\omega)]^2 + \omega^2 [\tilde{\varepsilon} - \beta(\omega)]^2}, \quad (6)$$

with

$$\alpha(\omega) = \omega K \frac{\sin(\omega\tau)(1-R)}{1 - 2R \cos \omega\tau + R^2}, \quad (7)$$

$$\beta(\omega) = K \frac{[1 - \cos(\omega\tau)](1+R)}{1 - 2R \cos \omega\tau + R^2}. \quad (8)$$

This analytical formula is in excellent agreement with numerical simulations (see Fig. 2). Note that for  $R$  close to unity (c) two main components can be clearly distinguished in the spectrum: a broad background, and a sharp peak on top of the background. The former hardly changes with varying  $R$ , whereas the latter sharpens as  $R$  increases. Since, according to the Wiener-Khinchin theorem, the power spectral density is the Fourier transform of the ACF, the spectral components reflect different time scales of the ACF. To separate those spectral components, we require  $1 - R \ll 1$ ,  $\tau \approx 2\pi n / \omega_0$ ,  $n \in \mathbb{N}$ , and consider Eq. (6) for two separate frequency domains:  $\omega\tau \approx 2\pi n$  and  $\omega\tau \neq 2\pi n$ . In the first case we set  $\omega = \omega_0(1 + \delta)$ , where  $\delta \ll 1$ . Taking into account that

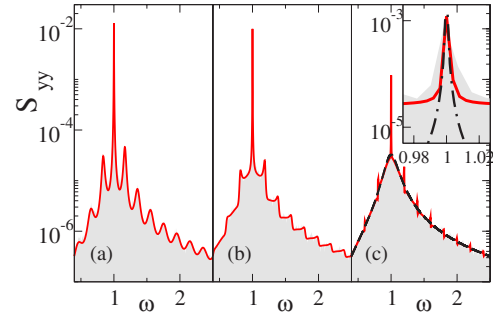


FIG. 2. (Color online) Spectrum of oscillations  $S_{yy}(\omega)$  of Eq. (1) for  $D=0.003$ ,  $K=0.2$ ,  $\tau=31.4$ : (a)  $R=0$ , (b)  $R=0.5$ , (c)  $R=0.9$  (inset: enlargement). Shaded: numerical simulation; solid line (red on-line): analytical result Eq. (6); dashed black line in (c): background approximation Eq. (10); dash-dotted line in inset of (c): peak approximation Eq. (9).

$\sin(\omega\tau) \approx \omega_0 \delta\tau$  and  $1 - \cos(\omega\tau) \approx (\omega_0 \delta\tau)^2 / 2$  [12], we obtain the approximation of Eq. (6),

$$S_{yy}^1(\omega) = \frac{D^2}{2\pi K^2 \tau^2} \frac{(1-R)^2}{(\omega - \omega_0)^2 + \left( \frac{\varepsilon(1-R)}{K\tau} \right)^2}, \quad (9)$$

in the vicinity of the sharp central peak. In the second case we rewrite  $1 - 2R \cos \omega\tau + R^2 = 2R(1 - \cos \omega\tau) + (1-R)^2$ . Noting  $(1-R)/2R \approx 0$ ,  $(1+R)/2R \approx 1$  we get

$$S_{yy}^2(\omega) = \frac{D^2}{2\pi} \frac{\omega^2}{(\omega^2 - \omega_0^2)^2 + \omega^2(\varepsilon - K)^2}, \quad (10)$$

which describes the background. The superposition  $S_{yy} \approx S_{yy}^1 + S_{yy}^2$  gives an approximation of Eq. (6), which, as Fig. 2(c) shows, quite accurately describes the spectrum for  $R$  close to unity, and  $\tau \approx 2\pi n / \omega_0$ . Thus, the origin of the two time scales of the ACF becomes clear. Since the ACF is the inverse Fourier transform of the power spectral density, it is the superposition of two terms, corresponding to the narrow peak  $S_{yy}^1$ , and the broad background  $S_{yy}^2$ , respectively.  $S_{yy}^1(\omega)$  is a Lorentzian with half-width  $\Gamma_1 = \varepsilon(1-R)/(K\tau)$ , yielding the Fourier transform  $\Psi_{yy}^1 \propto \exp(-\Gamma_1 t)$ . Hence, the slow exponential decay of the ACF with characteristic time  $t_e^1 = 1/\Gamma_1$  (Fig. 1) is defined by the width of the sharp spectral peak, whereas the broad background width  $\Gamma_2 = |\varepsilon - K|$  determines the abrupt drop of  $\Psi_{yy}^2 \propto \exp(-\Gamma_2 t/2)$  with characteristic time  $t_e^2 = 2/\Gamma_2$ . From Eq. (6) it follows that by variation of the control parameters  $K$ ,  $\tau$ ,  $R$  of the extended delayed feedback  $F$  one can control all essential features of noise-induced oscillations such as coherence, time scales, and spectral content. In particular, from Eqs. (9) and (10) it follows that by varying  $K$  one can control the short-term correlations, whereas  $R$  essentially governs long-term correlations.

In order to understand how the feedback  $F$  acts upon the long-term correlations, we examine the dependence of  $t_e \equiv t_e^1$  and  $S_{yy}$  upon the feedback parameters  $\tau$  and  $R$ . Figure 3(a) shows  $t_e$  vs time delay  $\tau$  for  $R=0.9$ , and  $K=0.2$ . Similarly to the case  $R=0$  [7,8,12,13], the minima of the correla-

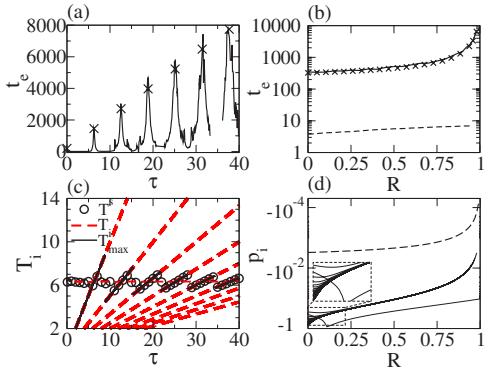


FIG. 3. (Color online) Exponential correlation time  $t_e$  (a) vs  $\tau$  for  $R=0.9$  and (b) vs  $R$  for  $\tau=6.28$  (solid line) and  $\tau=3.14$  (dashed line) and  $D=0.003$ ,  $K=0.2$ . The crosses mark the analytical estimate Eq. (17) for  $\tau=6.28$ ; (c) eigenperiods  $T_i=2\pi/q_i$  (dashed) where  $q_i$  are the imaginary parts of the eigenvalues  $\lambda_i$ , and largest spectral peak periods  $T^s$  (circles) vs  $\tau$  for  $R=0.9$ ; (d) real parts  $p_i$  of the eigenvalues  $\lambda_i$  given by the characteristic Eq. (11) vs  $R$  for  $\tau=6.28$  and  $K=0.2$ . Inset: lower real parts of eigenvalues in an enlarged scale.

tion time occur for  $\tau$  close to  $(2n-1)/2T_0$ , where  $n$  is an integer, and  $T_0=2\pi/\omega_0$  is the basic period of noise-induced oscillations for  $K=0$ , and the maxima occur for  $\tau=nT_0$ . A striking feature is, however, that for these optimal values of  $\tau$  the correlation time  $t_e$  increases dramatically with increasing  $R$  [see solid curve in Fig. 3(b)]. In fact, as  $R$  approaches unity,  $t_e \rightarrow \infty$ , i.e., by increasing  $R$  one can achieve practically any extent of coherence.

Some analytical insight into the mechanism of enhancement of the coherence can be obtained by noting that the stochastic oscillations occur in the vicinity of the fixed point  $(0,0)$ . Hence the stability properties of this fixed point influence the noise-induced dynamics. To check this assumption a linear stability analysis is performed. The characteristic equation corresponding to Eqs. (1) with  $D=0$  linearized around the origin reads

$$\lambda^2 - \varepsilon\lambda + \omega_0^2 + K\lambda \frac{1 - e^{-\lambda\tau}}{1 - Re^{-\lambda\tau}} = 0. \quad (11)$$

Due to the delay term, this equation yields a countable set of complex eigenvalues  $\lambda_k = p_k + iq_k$  with real  $p_k, q_k$ . First, we check if the delayed feedback induces a Hopf bifurcation, which would provide a trivial explanation for the enhancement of regularity of oscillations. Setting  $p_k=0$  and  $q_k \neq 0$ , and splitting Eq. (11) into real and imaginary parts, we obtain the condition

$$\cos(q_k\tau) = \frac{K + KR - (1 + R^2)\varepsilon}{K + KR - 2R\varepsilon}. \quad (12)$$

Since  $\varepsilon < 0$ ,  $K > 0$ ,  $R \geq 0$ , and  $|\cos(q_k\tau)| \leq 1$ , this equation cannot be satisfied for  $1 + R^2 > 2R$ , which is equivalent to  $(R-1)^2 > 0$ . Thus, for  $0 \leq R < 1$  the feedback cannot induce a Hopf bifurcation, and the real parts  $p_k$  always remain negative.

The solution of Eq. (11) is shown in Figs. 3(c) and 3(d). The enhancement in the regularity of noise-induced oscillations is connected with the eigenvalue, which has the largest real part  $p_{max} < 0$ . Namely, if a real part  $p_k$  comes close to 0, the corresponding eigenmode becomes less stable and can be excited more easily by noise, which leads to more regular oscillations. For optimum  $\tau \approx nT_0$ , where  $n$  is an integer, and  $R \rightarrow 1$ , the largest eigenvalue tends to 0, thus inducing a dramatic increase of the correlation time [Fig. 3(b)]. We also note that a crossover between different modes  $p_k$  results in a jump in the characteristic period of noise-induced oscillations with increasing  $\tau$  as in the case  $R=0$  [7]. As is shown in Fig. 3(c), the eigenperiod  $T_{max}=2\pi/q_{max}$  corresponding to the largest real part (solid line) agrees with the period  $T^s$  of the main peak of the spectrum (circles) and depends piecewise linearly on  $\tau$ .

Now let us analytically estimate the correlation time  $t_e$ . In [13] it has been shown that for  $R=0$ , small  $D$  and  $\tau$  close to  $nT_0$ ,  $t_e$  is related to the largest real part  $p_{max}$  of the eigenvalues

$$t_e \approx -\frac{1}{p_{max}}. \quad (13)$$

The key idea for the derivation of the above relation is to neglect all but the least stable eigenmode of the system, thereby approximating the Van der Pol system by a two dimensional Ornstein-Uhlenbeck process [13]. This assumption is justified if only one real part  $p_{max}$  of the eigenvalues is close to 0 and all others have an absolute value, which is at least one order of magnitude larger. As it is seen from Fig. 3(d), this assumption is also valid for  $R > 0$ . Then the corresponding eigenvalue  $\lambda_{max} = p_{max} + iq_{max}$  can be rewritten as

$$\lambda_{max} = \delta_p + i(1 + \delta_q)\omega_0, \quad (14)$$

where  $|\delta_p|, |\delta_q| \ll 1$ . Substitution of  $e^{-\lambda\tau} = 1 - \lambda\tau + \mathcal{O}(\lambda^2)$  in Eq. (11) and neglecting the terms of higher order yields

$$Ki\omega_0(1 - e^{-i\omega_0\tau} + e^{-i\omega_0\tau}\tau\Lambda) + K\Lambda(1 - e^{-i\omega_0\tau}) + (1 - Re^{-i\omega_0\tau})(2i\omega_0\Lambda - i\varepsilon\omega_0) = 0, \quad (15)$$

with  $\Lambda = \delta_p + i\delta_q\omega_0$ . For the optimum  $\tau = 2\pi n/\omega_0$  the solution of this equation can be found exactly:

$$p_{max} = \frac{\varepsilon}{2} \frac{1}{1 + \frac{K}{2(1-R)}\tau}, \quad q_{max} = \omega_0. \quad (16)$$

Then from Eq. (13) we obtain the correlation time

$$t_e = -\frac{2}{\varepsilon} \left( 1 + \frac{K}{2(1-R)}\tau \right). \quad (17)$$

Figures 3(a) and 3(b) show that this result is in very good agreement with the numerical simulations. As  $R \rightarrow 1$  we have  $t_e \rightarrow \infty$ , which means that the correlation time can be increased arbitrarily. It should be noted that for  $R$  close to unity the formula (17) becomes equal to  $t_e^1 = 1/\Gamma_1$ , which is the inverse width of the sharp central peak of the spectrum (6) in the approximation (9).

Finally, the stability and the frequency of all eigenmodes in dependence on  $R$  gives us detailed insight into the decomposition of the spectrum into a flat background and a sharp peak and thus into the origin of the different time scales of the ACF. The numerical solution of the characteristic equation shows that the imaginary parts (i.e., the frequency) of the eigenvalues remain practically constant with increasing  $R$ . Therefore the frequencies of the spectral peaks do not change with increasing  $R$  (see Fig. 2). Inspection of the stability of different eigenmodes [Fig. 3(d)] reveals the following effect of the multiple-time delayed feedback: For optimum  $\tau$  the largest real part of the eigenvalues tends to 0 for  $R \rightarrow 1$ . This leads to the increasing correlation time and the sharp peak in the spectrum. The real parts of all other eigenmodes that are generated by the delayed feedback loop approach each other as  $R$  increases. Hence white noise can equally well excite all eigenmodes due to their comparable stability features. Since, however, they all have different frequencies we obtain the flat background in the spectrum. For  $R \rightarrow 1$  these real parts also tend to 0 like the largest real part. This means that, concomitant with a sharper main peak, we also get an increasing background in the spectrum.

In conclusion, we have shown that extended multiple-time delayed feedback leads to an interesting phenomenon in the control of noise-induced oscillations near a Hopf instability:

It creates two distinct, independent time scales in the auto-correlation function, and allows for a dramatic increase of the correlation time, as compared to single-time delayed feedback control. The long-term correlations are essentially controlled by the memory parameter  $R$ . The most coherent oscillations occur for  $\tau$  close to an integer multiple of the basic period of noise-induced oscillations without control. The possibility to increase the correlation time to arbitrarily large values by tuning  $R$  opens up new applications. Since our results are derived for the paradigmatic Van der Pol system (which is representative for nonlinear oscillators close to a Hopf bifurcation), this control method promises wide applicability in physics, chemistry, biology, medicine, technology, where it is often not sufficient to tune the coherence properties of noise-driven dynamics only slightly, but where there is need to improve the coherence by many orders of magnitude. It seems promising to apply multiple-time delayed feedback also to systems of coupled stochastic oscillators [15] describing neural dynamics, and space-time patterns in reaction-diffusion systems [16] to drastically improve single-time control methods.

This work was supported by DFG in the framework of Sfb 555 and by EPSRC (UK).

- 
- [1] R. Benzi, A. Sutera, and A. Vulpiani, *J. Phys. A* **14**, L453 (1981).
  - [2] Hu Gang, T. Ditzinger, C. Z. Ning, and H. Haken, *Phys. Rev. Lett.* **71**, 807 (1993).
  - [3] A. S. Pikovsky and J. Kurths, *Phys. Rev. Lett.* **78**, 775 (1997).
  - [4] V. S. Anishchenko, A. B. Neiman, F. Moss, and L. Shimansky-Geier, *Phys. Usp.* **42**, 7 (1999).
  - [5] B. Lindner, J. García-Ojalvo, A. Neiman, and L. Shimansky-Geier, *Phys. Rep.* **392**, 321 (2004).
  - [6] D. J. Christini and J. J. Collins, *Phys. Rev. Lett.* **75**, 2782 (1995).
  - [7] N. B. Janson, A. G. Balanov, and E. Schöll, *Phys. Rev. Lett.* **93**, 010601 (2004).
  - [8] A. G. Balanov, N. B. Janson, and E. Schöll, *Physica D* **199**, 1 (2004).
  - [9] J. E. S. Socolar, D. W. Sukow, and D. J. Gauthier, *Phys. Rev. E* **50**, 3245 (1994).
  - [10] S. Schikora, P. Hövel, H.-J. Wünsche, E. Schöll, and F. Henneberger, *Phys. Rev. Lett.* **97**, 213902 (2006).
  - [11] K. Pyragas, *Phys. Lett. A* **170**, 421 (1992).
  - [12] E. Schöll, A. Balanov, N. B. Janson, and A. Neiman, *Stochastics Dyn.* **5**, 281 (2005).
  - [13] J. Pomplun, A. Amann, and E. Schöll, *Europhys. Lett.* **71**, 366 (2005).
  - [14] C. W. Gardiner, *Handbook of Stochastic Methods for Physics, Chemistry and the Natural Sciences* (Springer, Berlin, 2002).
  - [15] B. Hauschildt, N. B. Janson, A. Balanov, and E. Schöll, *Phys. Rev. E* **74**, 051906 (2006).
  - [16] G. Stegemann, A. G. Balanov, and E. Schöll, *Phys. Rev. E* **73**, 016203 (2006); A. G. Balanov, V. Beato, N. B. Janson, H. Engel, and E. Schöll, *ibid.* **74**, 016214 (2006).